ADVANCED OPTICAL MATERIALS

Supporting Information

for *Adv. Optical Mater.*, DOI 10.1002/adom.202202851

Unveiling the Transformation from Aggregation-Caused Quenching to Encapsulation-Induced Emission Enhancement for Improving the Photoluminescence Properties and Detection Performance of Conjugated Polymer Material in Multiple States

Sameer Hussain, Xi Chen, Yingying Gao, Huijia Song, Xuemeng Tian, Yulian He, Ansar Abbas, Mohammad Adil Afroz, Yi Hao and Ruixia Gao**

Supporting Information

Unveiling ACQ-to-EIEE Transformation for Augmenting Photoluminescent Properties and Improving Detection Performance of Conjugated Polymer Material in Multiple States

Sameer Hussain, Xi Chen, Yingying Gao, Huijia Song, Xuemeng Tian, Yulian He, Ansar Abbas, Mohammad Adil Afroz, Yi Hao, and Ruixia Gao**

EXPERIMENTAL SECTION

Materials and Measurements: Pluronics viz. L–64, L–35 and F–108 were purchased from Aladdin. Pluronics F–127 and F–68 were acquired from Sigma–Aldrich and Macklin. Tetracyclines were bought from Macklin as their corresponding salts. All other chemicals and reagents including were purchased from Merck, Aladdin, Macklin and used as received. Absorption and emission spectra were measured on a UV–2450 (Shimadzu) and F–2700 (Hitachi, Japan) spectrophotometer using quartz cuvettes with 10 mm path length and a slit width of 2 nm at room temperature. Ultrapurified water (18 MΩ/cm) was obtained using WaterPro system (Axlwater Corporation, TY10AXLC1805-2, China) and used throughout the experiments. The morphological studies were carried out using Gemini SEM 500 field emission scanning electron microscope (FE–SEM) (Carle Zeiss Management Co., Ltd.,

Germany) with silicon wafer as the substrate and JSM–2100 transmission electron microscope (TEM) (Jeol Ltd., Japan). Transmission electron microscope/energy-dispersive X-ray spectrometry (TEM-EDS) was recorded by a Tecnai G2 F20 microscope (USA). Fluorescence microscopic images were captured using fluorescence microscope (Olympus, Tokyo, Japan). Time–resolved fluorescence measurements were performed using FLS980 Spectrometer (Edinburgh Instrument, UK). Photos of the sample solutions were taken using a Nikon D–750 camera under a UV lamp (365 nm excitation). Cyclic voltammetry was performed using electrochemical workstation of CH instruments Model 660D series.

Synthesis of Precursor Polymer PF–DBT–Br: Conjugated Polymer PF–DBT–Br was prepared using our previously established procedure.[1,2]. In brief, monomers M1, M2 and M3 with a mole ratio of 0.45:0.50:0.05 were dissolved well in THF (30 mL) and placed to a double neck flask. The reaction mixture was properly degassed followed by insertion of 2M aq. K_2CO_3 (5ml) under continuous stirring. Then, $Pd(PPh_3)_4$ catalyst was introduced into the reaction mixture followed by refluxing under inert atmosphere with continuous stirring for 48 h. The solvent was then evaporated under reduced pressure and the mixture was extracted thrice using chloroform and water. The organic layer was dried using anhy. Mg_2SO_4 to obtain pink colored residue. The residue was dissolved in minimum chloroform followed by multiple precipitations in methanol and acetone to get pure brominated polymer PF–DBT–Br as pinkish–red colored compound. ^{1}H NMR (400 MHz, $CDCl_3$): δ 8.18–6.86 (b, aromatic backbone), 3.40–3.10 (b, Br–C**H**$_2$–$(CH_2)_5$), 2.25–0.60 (b, Br–CH_2–(C**H**$_2$)$_5$).

Synthesis of Cationic Conjugated Polymer PF–DBT–Im: Conjugated Polymer PF–DBT–Im was synthesized following our earlier protocol.[2] The brominated polymer PF–DBT–Br (50

mg) was dissolved in dichloromethane (10 mL) and transferred to a flask containing excess of N–methyl imidazole (5 mL). After continuously stirring the reaction mixture at room temperature for 2 days, dichloromethane was removed under reduced pressure. The reaction mixture was then diluted with methanol and undergoes purification by dialysis using a cellulose membrane with molecular weight cut–off 2.5 kDA. The acquired polymer was then concentrated and washed repeatedly with dichloromethane to eliminate any unreacted brominated polymer. After vacuum drying, the desired conjugated polymer PF–DBT–Im was acquired as dark pink colored product. ^{1}H NMR (400 MHz, *d6*-DMSO): δ 9.65–9.55 (b, N=C**H**–N), δ 9.30–9.01 (b, N–C**H**=C**H**–N), δ 8.30–6.70 (b, aromatic backbone), 4.15–4.04 (b, N–C**H**$_2$–(CH$_2$)$_5$), 3.90–3.70 (b, N–C**H**$_3$), 2.25–0.40 (b, N–CH$_2$–(C**H**$_2$)$_5$).

Synthesis of Conjugated Polymers PF-BT-Im and PF-DBT-COONa: Conjugated polymers PF-BT-Im and PF–DBT–COONa were synthesized using reported procedures.[2-3]

Determination of Photoluminescence Quantum Yield (PLQY): Firstly, the fluorescence quantum yield (Φ_s) of polymer PF–DBT–Im alone was measured[4] in water using the below equation taking quinine sulfate (Φ_r = 0.54 in 0.1 M H_2SO_4) as standard-

$$\Phi_s = \Phi_r (A_r F_s / A_s F_r) (\eta_s^2 / \eta_r^2)$$

where Φ signifies fluorescence quantum field, A_s and A_r represents absorbance value of standard and PF–DBT–Im, F_s and F_r denotes integrated fluorescence intensity of PF–DBT–Im and standard under excitation value of 365 nm, η indicates refractive index of the medium used. To minimize the error due to re–absorption effects, the absorbance value of standard and PF–DBT–Im solution were adjusted less than 0.1 at the excitation wavelength. The wavelength of 365 nm was chosen as moderate excitation wavelength considering excitation

wavelengths of quinine sulfate standard and PF–DBT–Im as ~350 nm and ~380 nm, respectively. Following the same procedure, the fluorescence quantum yield of PF–DBT–Im was also calculated in the presence of various Pluronics (37 °C) and hydrogel (RT) using their micellar and gelation concentrations.

Absorption and Photoluminescence Studies: For comparing fluorescence enhancement of PF–DBT–Im with various Pluronics, PF–DBT–Im (10 μM) was introduced into 10 mM HEPES (pH=7.4) containing micellar concentrations of L–64 (0.8 mM), L–35 (5.5 mM), F–127 (10 μM), F–68 (0.6 mM) and F–108 (100 μM), respectively in a quartz cuvette of 10 mm width. The emission spectra were then monitored after vigorously shaking the solutions for 10 min at 37 °C using excitation wavelength of 380 nm. The sensing studies were performed by adding TCs in portions separately to the solution of PF–DBT–Im/Pluronic F–127 (10 μM/10 μM) in 10 mM HEPES buffer (pH=7.4) keeping the total volume same at each time and monitoring emission spectra at 37 °C. For comparative studies, PF–DBT–Im (10 μM) solution in the absence of Pluronic F–127 was also employed for the detection of TCs. For selectivity studies, various common drugs (streptomycin, lincomycin, ampicillin, chloramphenicol, sulfamethoxazole, erythromycin, sulfdiazine), metal ions (Cu^{2+}, Cd^{2+}, Co^{2+}, Cr^{3+}, Mg^{2+}), anions (Cl^{-}, SO_4^{2-}, CH_3COO^{-}, CO_3^{2-}, $C_2O_4^{2-}$) and amino acids (histidine, cysteine, valine, tryptophan, isoleucine) were added at a concentration of 100 μM to the solution of PF–DBT–Im/Pluronic F–127 (10 μM/10 μM) separately and change in emission spectra was monitored. For UV–visible absorption studies, change in absorbance of PF–DBT–Im/Pluronic F–127 (10 μM/10 μM) was monitored at 37 °C by sequentially introducing increasing concentrations of each TCs separately in 10 mM HEPES buffer (pH=7.4) keeping the total volume same each time.

Stern–Volmer Quenching Constant (K_{sv}) and Detection Limit (LOD) Calculations: The quenching constant (K_{sv}) values for each tetracycline antibiotics were determined[4] from the slope of regression curve equation attained by plotting I_0/I vs [TCs]. Here, I_0 represents fluorescence intensity (at 415 nm) of PF–DBT–Im/Pluronic F–127 solution in the absence of TC and I indicate the intensity of PF–DBT–Im/Pluronic F–127 solution at particular TC concentration. Likewise, LOD for each TC was calculated using the established equation[4]–

$$LOD = 3 \times \sigma/K$$

where, K signifies the slope of regression curve equation acquired by plotting the change in emission intensity (at 415 nm) of PF–DBT–Im/pluronic F–127 against the concentration of respective TC, σ indicates the standard deviation of the emission intensity of PF–DBT–Im/Pluronic F–127 in the absence of TC. For comparison, similar procedure was employed to calculate K_{sv} and LOD values for TCs using PF–DBT–Im solutions in the absence Pluronic F–127.

Time-Resolved Photoluminescence Spectroscopy (TRPL): To study the fluorescence lifetime decay of PF–DBT–Im/Pluronic F–127 (10 μM/10 μM) micelles in the absence and presence of TCs (50 μM), time–correlated single–photon counting (TCSPC) measurements were performed. UV laser source with pulse excitation (375 nm) was employed to monitor emission counts (415 nm). The acquired curves in each case were fitted bi–exponentially followed by calculation of average lifetime (τ_{avg}) using the below equation–

$$\tau_{avg} = \frac{\sum_{i=1}^{n} a_i \, {\tau_i}^2}{\sum_{i=1}^{n} a_i \, \tau_i}$$

where, a_i and τ_i represents the amplitude and lifetime of i^{th} component.

Correction Method for Inner Filter Effect (IFE)

The role of IFE in suppressing the emission intensities of PF–DBT–Im and PF–DBT–Im/Pluronic F–127 after addition of TCs was assessed by performing the corrections using the standard equation shown below–

$$\frac{I_{corr}}{I_{obs}} = 10^{(A_{ex}+A_{em})/2}$$

where, I_{corr} and I_{obs} represent emission intensities after and before the correction, A_{ex} and A_{em} signifies the corresponding absorbance values at excitation and emission wavelength.

Electrochemical measurements

Cyclic voltammetry was carried out using three–electrode system at room temperature under inert atmosphere using N_2. Platinum sheet was used as counter electrode, the saturated Ag/Ag^+ was used as reference electrode and a glassy carbon was used as working electrode, respectively. PF–DBT–Im was drop–casted on working electrode as thin film from its alcoholic solution. The Fc^+/Fc couple was used as an internal reference using $TBAPF_6$ (0.1 M) as supporting electrolyte in acetonitrile. HOMO and LUMO energy levels were determined through onset calculation according to the following standard equation[3]–

$$E_{HOMO} = -(E_{oxid\ onset\ (PF\text{-}DBT\text{-}Im)} - E_{oxid\ onset\ (Fc)} + 4.8)\ eV$$

$$E_{LUMO} = -(E_{red\ onset\ (PF\text{-}DBT\text{-}Im)} - E_{red\ onset\ (Fc)} + 4.8)\ eV$$

Preparation of Hybrid Hydrogels

To attain EIEE–active fluorescent hydrogel, PF–DBT–Im (10 µM) was mixed into 1 ml cold solution of Pluronic F–127 (20% w/v) and F–108 (20% w/v) prepared separately in glass vials. The mixtures were kept in refrigerator again for ~30 minutes to realize complete

dissolution and proper mixing of Pluronic F–127 with PF–DBT–Im into aqueous solution. Afterwards, the glass vial containing solution was removed and allowed to reach room temperature. Once the temperature reached above 15 ºC, highly viscous bright fluorescent hybrid hydrogel was obtained. The hybrid fluorescent hydrogel showed reversible gel–sol behavior on cooling. ACQ–active hydrogel were prepared by doping of PF–DBT–Im (10 µM) into 5% (w/v) solutions of chitosan and hyluronic acid, respectively.

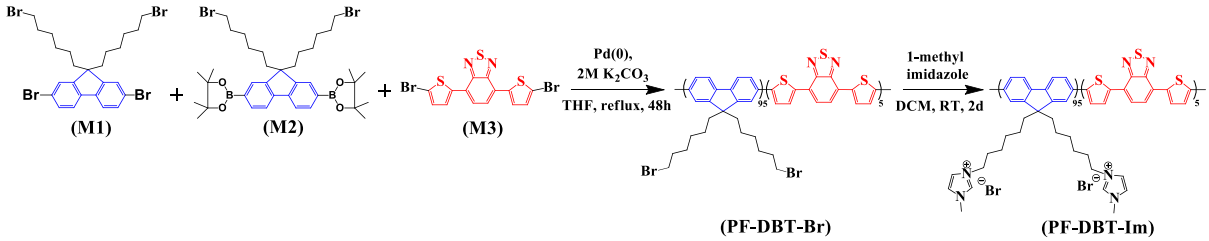

Scheme S1. Synthetic scheme for cationic conjugated polymer PF–DBT–Im.

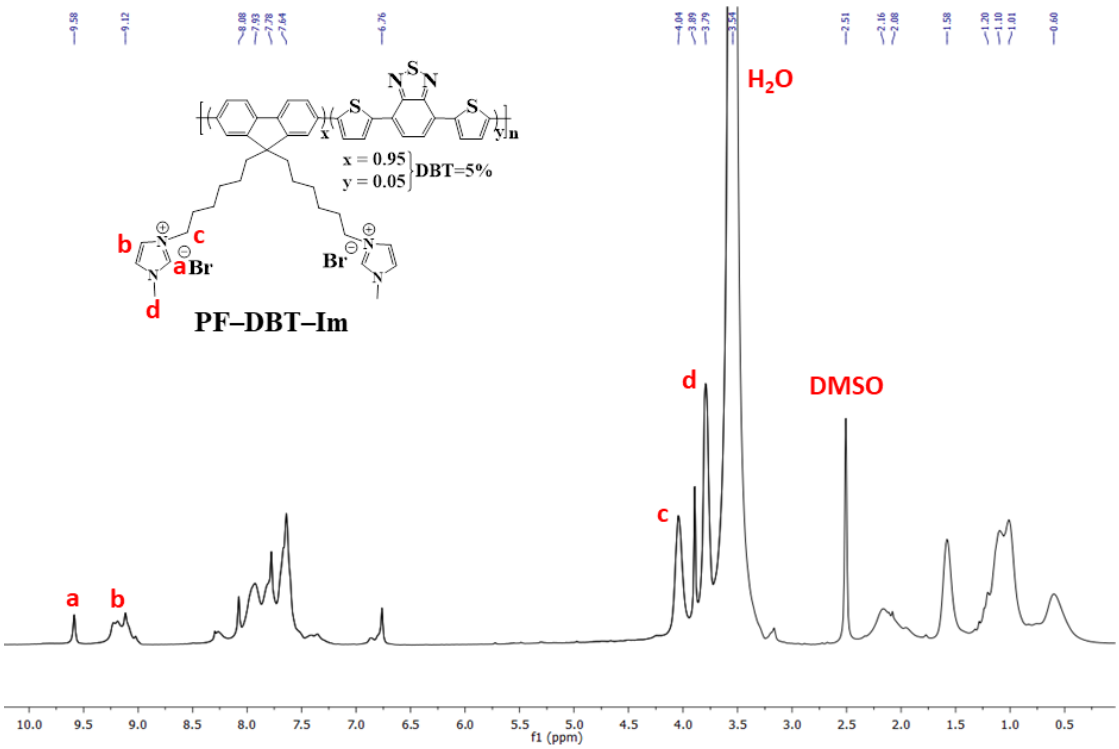

Figure S1. ^{1}H-NMR spectrum of polymer PF-DBT-Im.

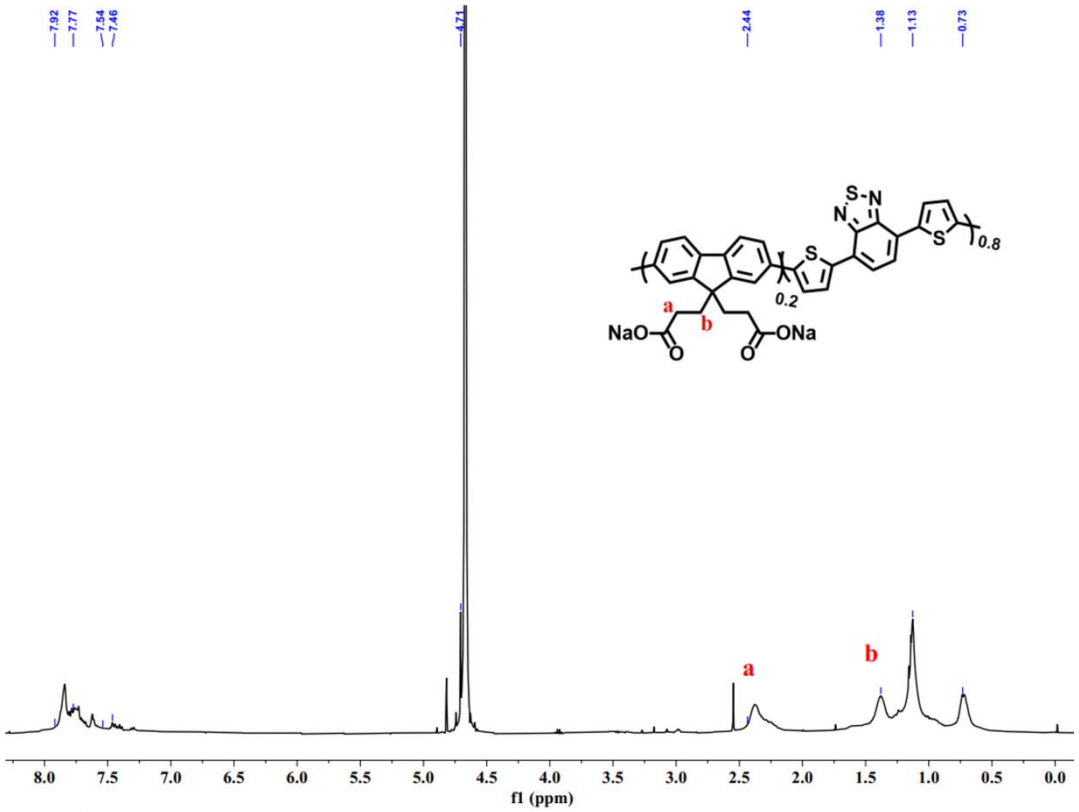

Figure S2. [1]H-NMR spectrum of polymer PF-DBT-COONa.

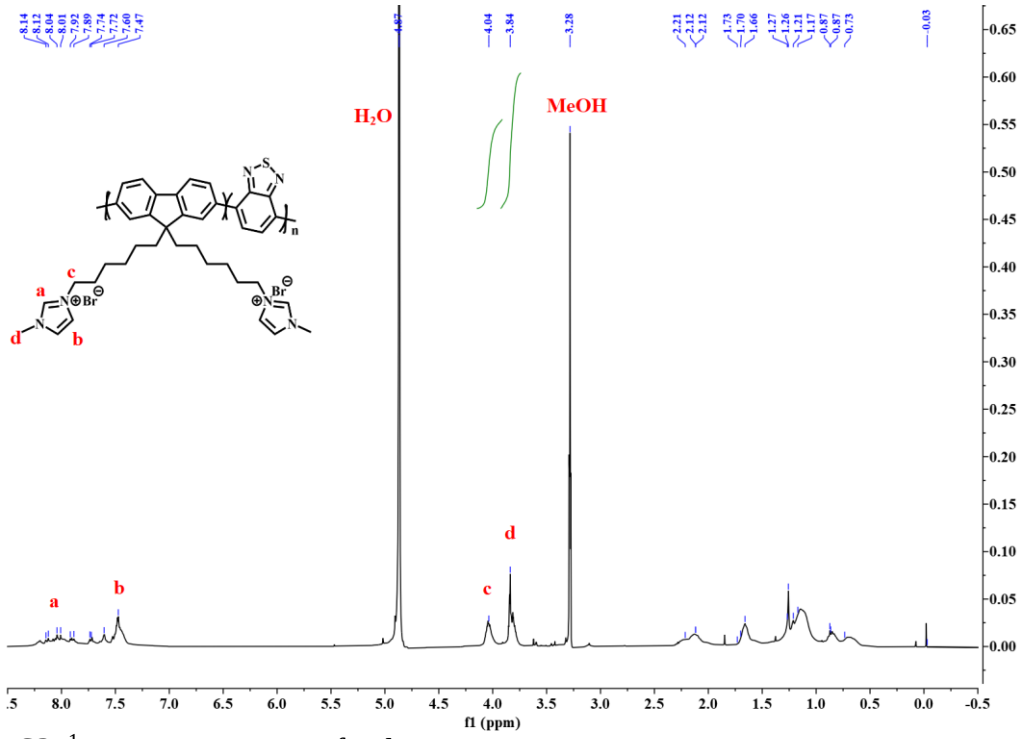

Figure S3. [1]H-NMR spectrum of polymer PF-BT-Im

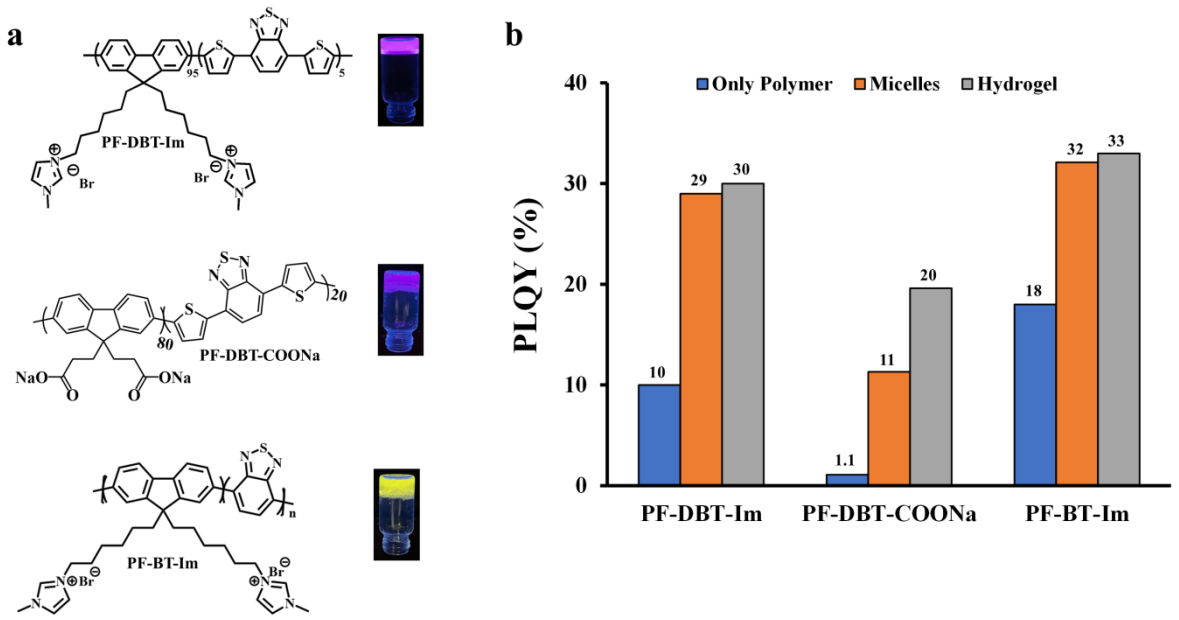

Figure S4. (a) Structures of different low water dispersible conjugated polymers employed in the present study and images (under UV-lamp irradiation) of corresponding fluorescent hybrid hydrogels prepared using F-127. (b) PLQY of different conjugated polymers in various states.

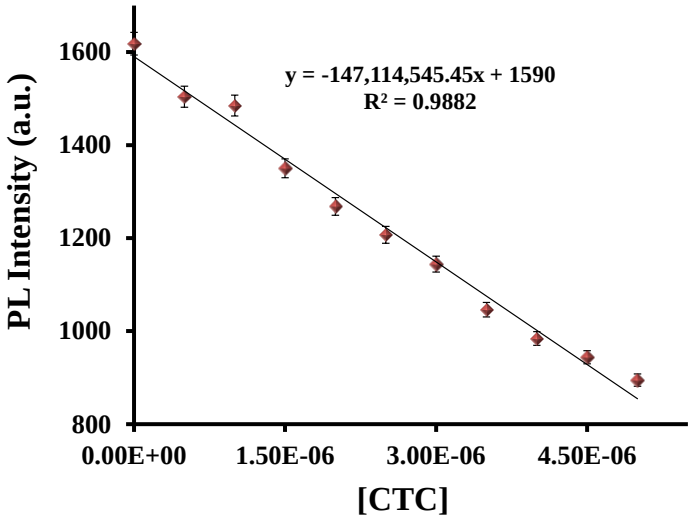

Figure S5. Detection limit plot for CTC.

LOD =3 × S.D./k

LOD = 3 × 12.39/147114545.45

= 2.52 × 10^{-7} M (129 ppb)

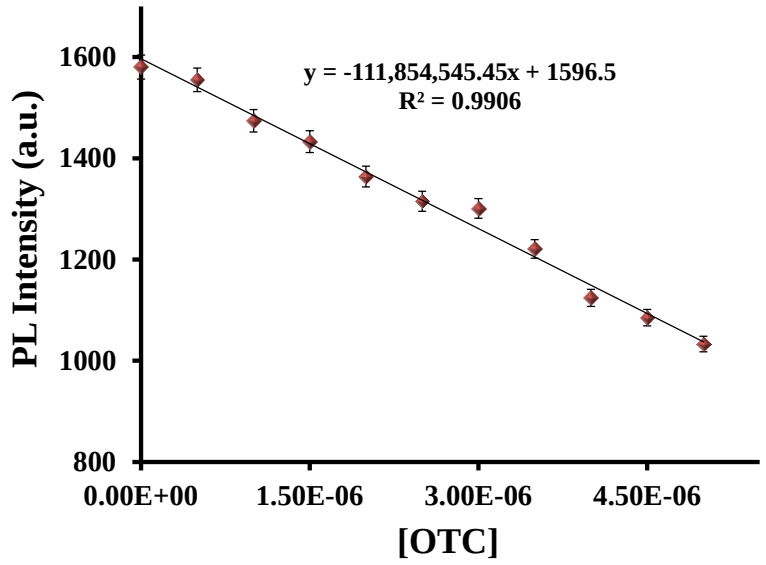

Figure S6. Detection limit plot for OTC.

LOD =3 × S.D./k

LOD = 3 × 11.43/111854545.45

= 3.06× 10^{-7} M (154 ppb)

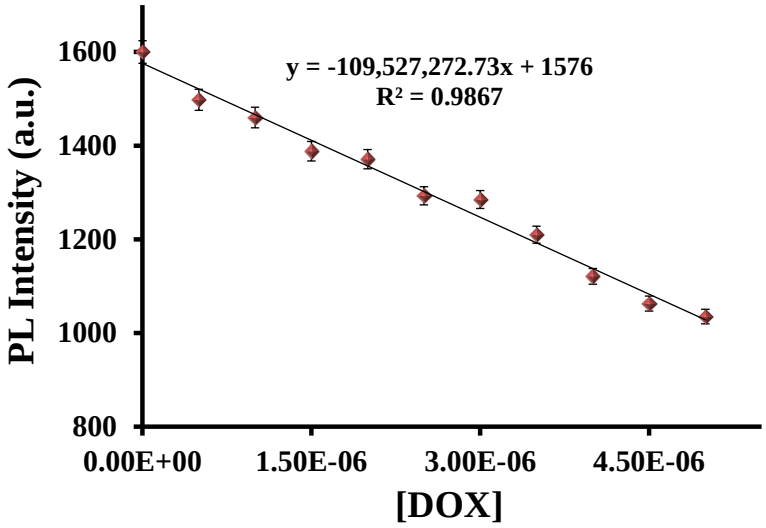

Figure S7. Detection limit plot for DOX.

LOD =3 × S.D./k

LOD = 3 × 12.08/109527272.73

= 3.31× 10^{-7} M (159 ppb)

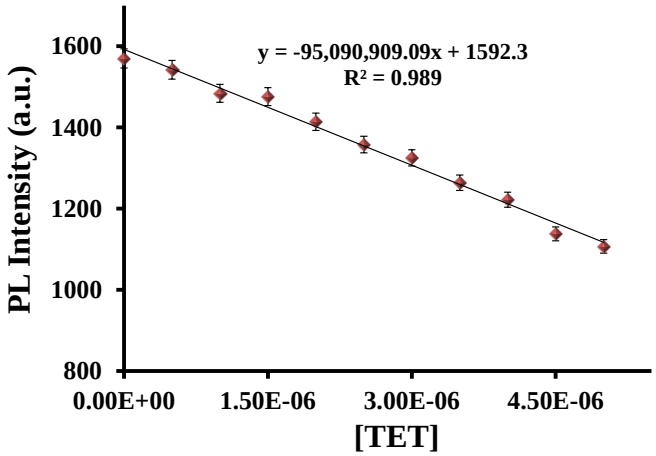

Figure S8. Detection limit plot for TET.

LOD =3 × S.D./k

LOD = 3 × 12.55/95090909.09

= 3.96× 10^{-7} M (192 ppb

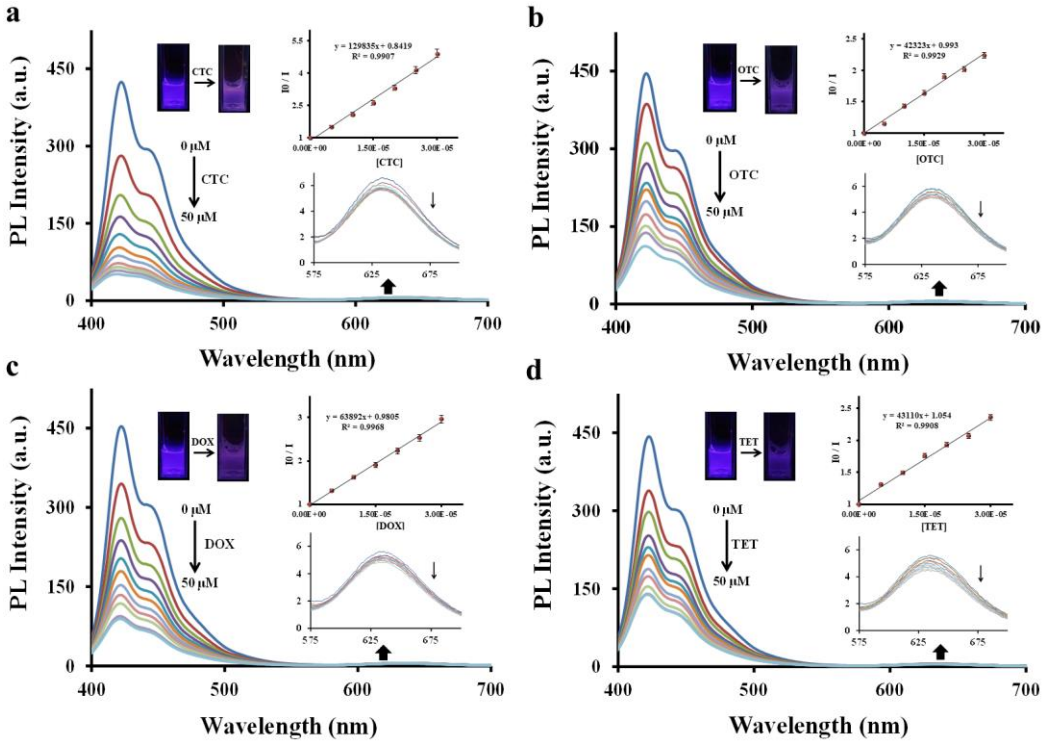

Figure S9. Emission spectra of PF–DBT–Im (10 µM) with increasing concentration of (a) CTC (b) OTC, (c) DOX and (d) TET, respectively. Inset: Corresponding change in emission color of solution under UV light and K_{sv} plot.

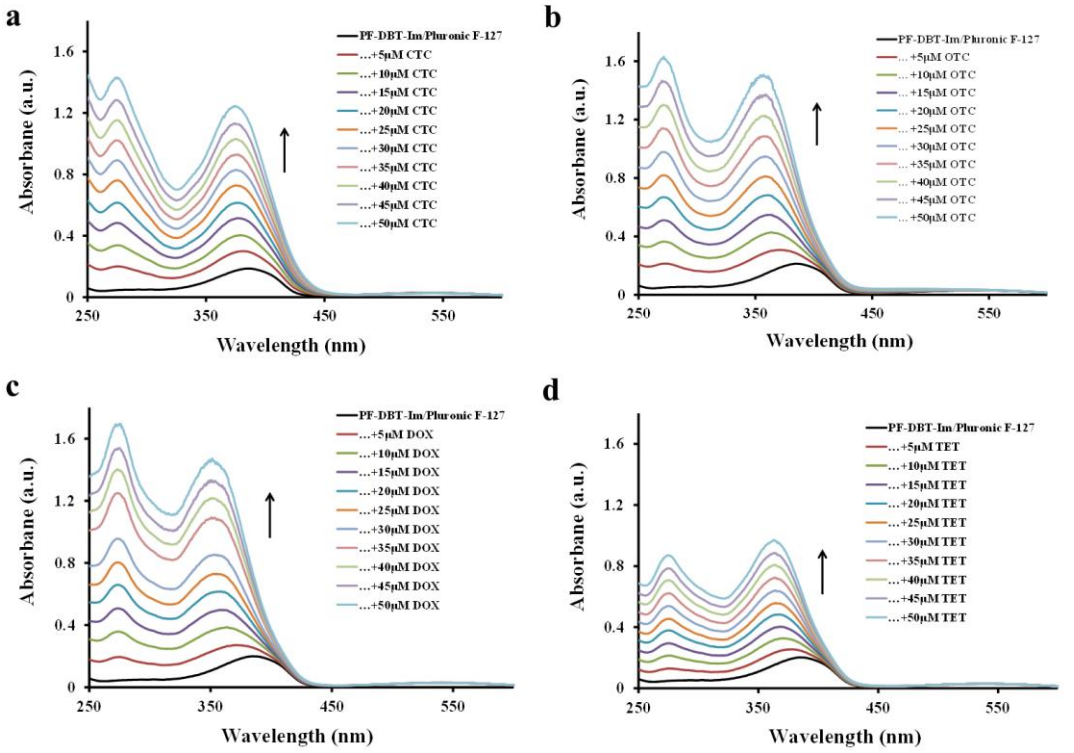

Figure S10. Change in absorption spectra of PF–DBT–Im/Pluronic F–127 (10 μM/10 μM) with increasing concentration of (a) CTC, (b) OTC, (c) DOX and (d) TET, respectively in 10 mM HEPES (pH=7.4).

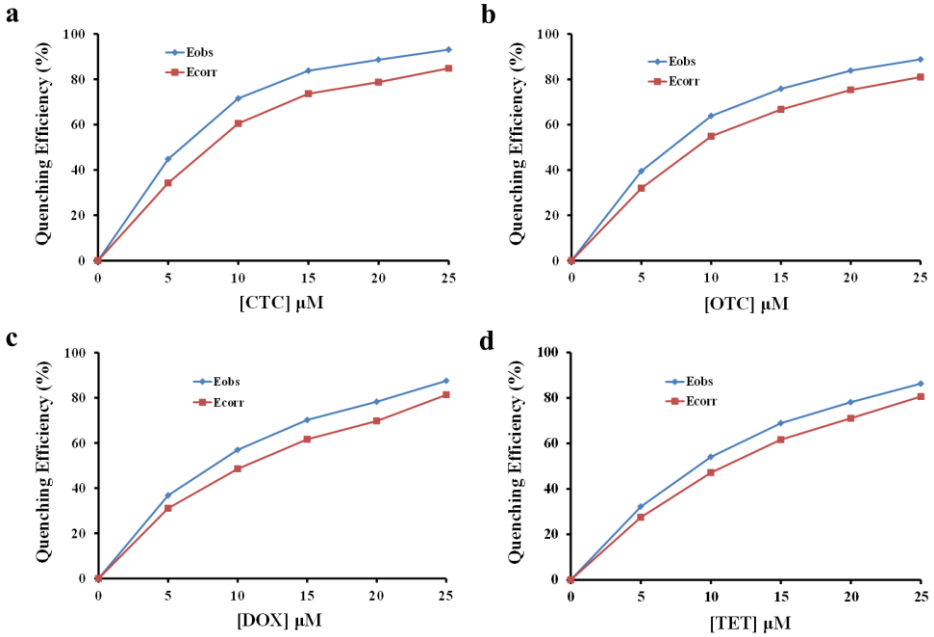

Figure S11. IFE correction plots of PF–DBT–Im/Pluronic F–127 (10 μM/10 μM) for different TCs.

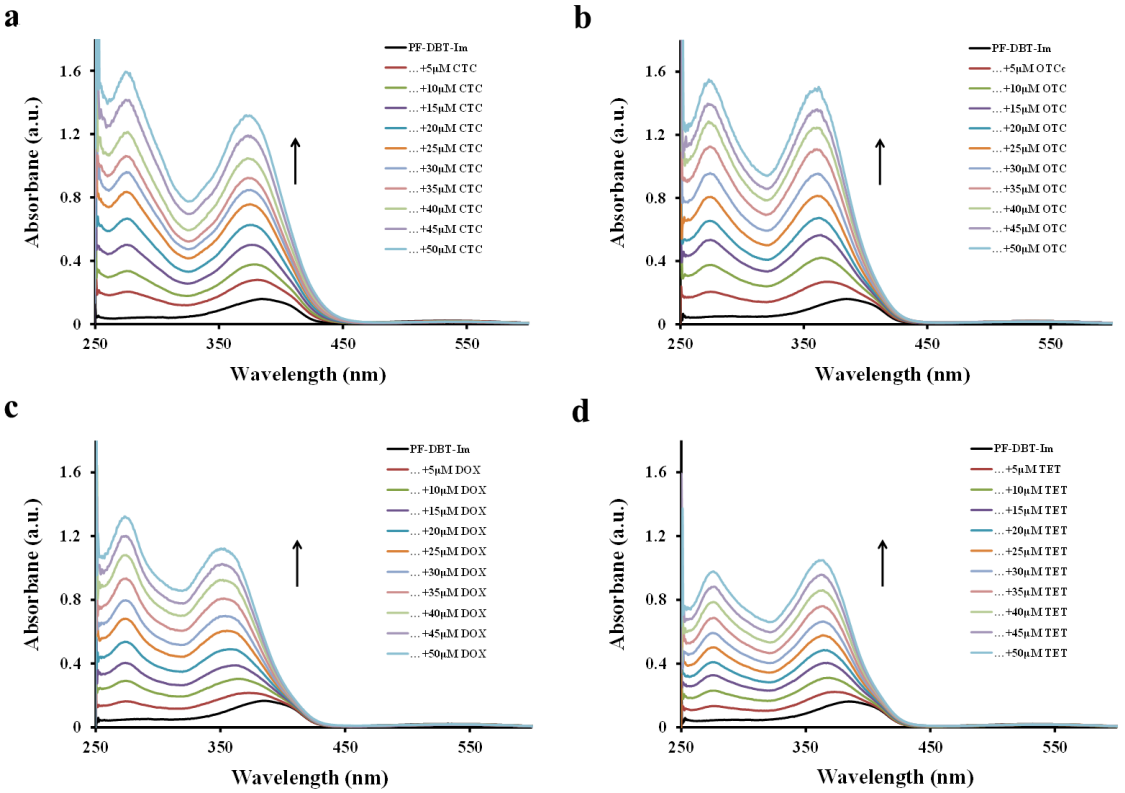

Figure S12. Change in absorption spectra of PF–DBT–Im (10 μM) with increasing concentration of (a) CTC, (b) OTC, (c) DOX and (d) TET, respectively.

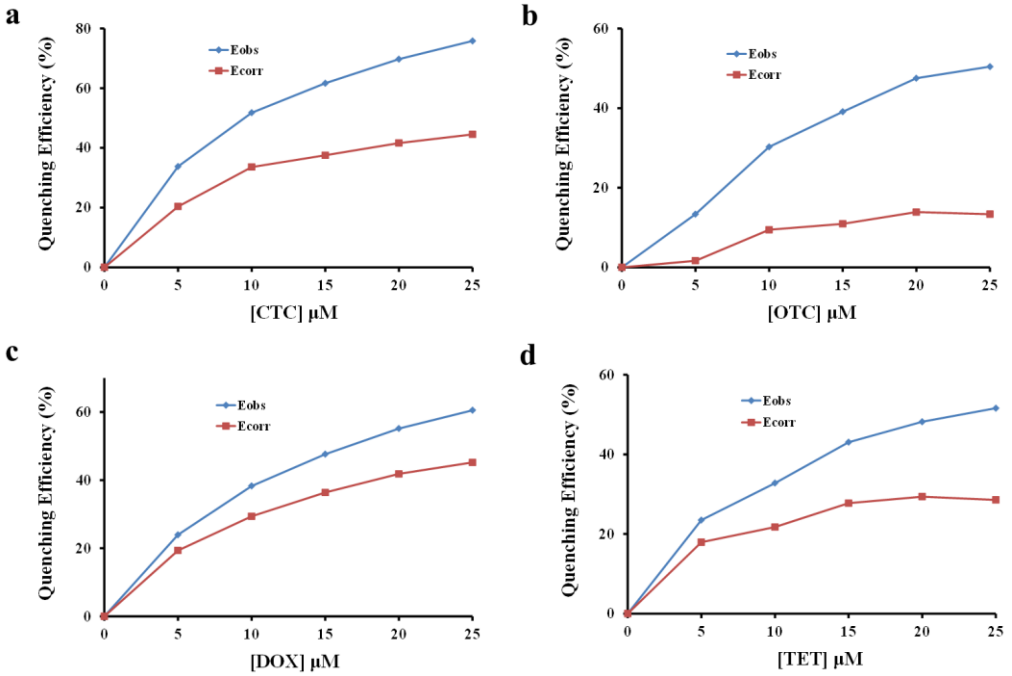

Figure S13. IFE correction plots of PF–DBT–Im (10 μM) for different TCs.

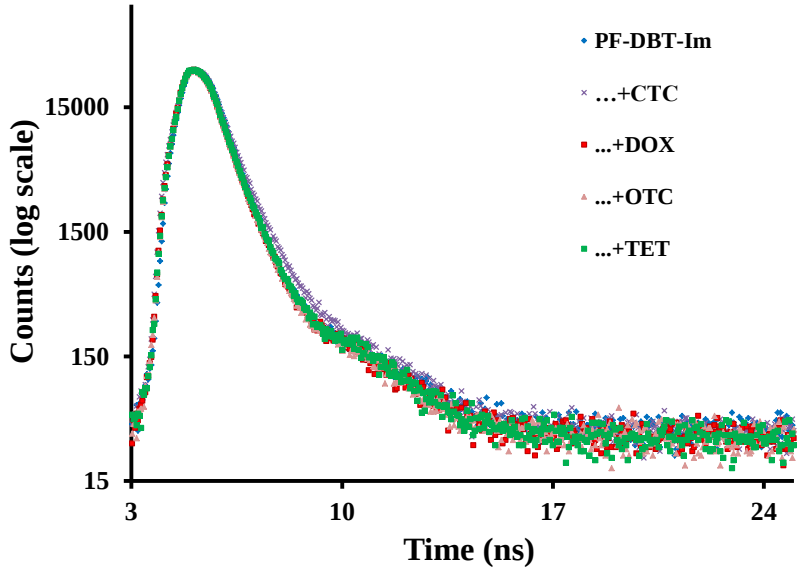

Figure S14. Change in lifetime decay of PF–DBT–Im with different TCs.

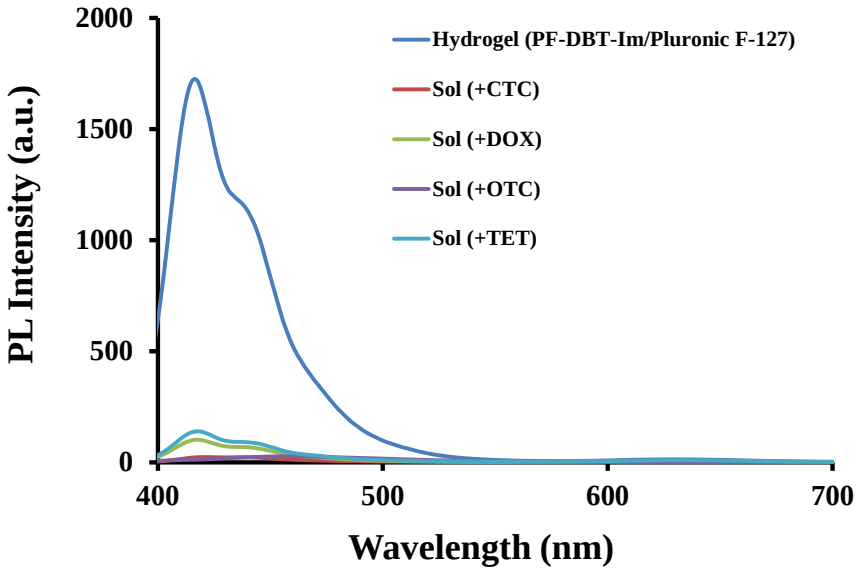

Figure S15. Change in emission intensity PF–DBT–Im/Pluronic F–127 hydrogel after addition of TCs (100 μM).

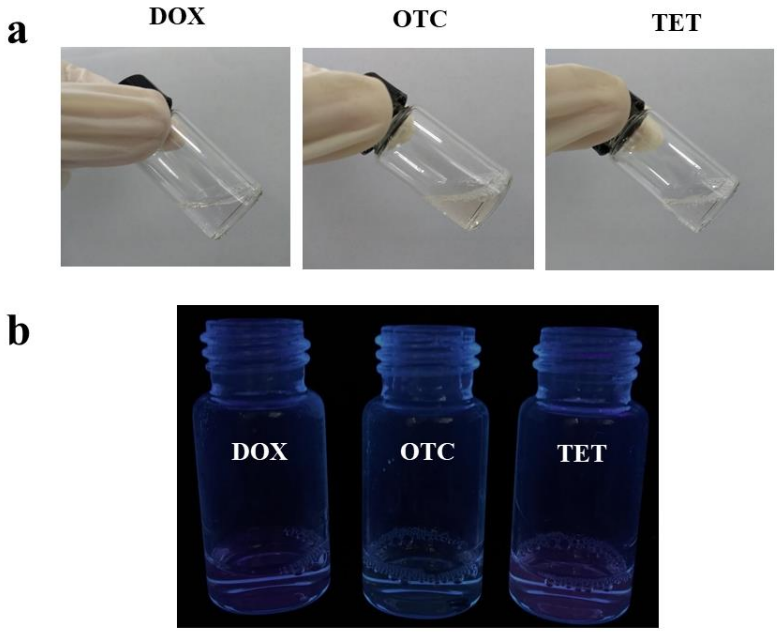

Figure S16. (a) Abolition and (b) fluorescence quenching of EIEE–active PF–DBT–Im/Pluronic F–127 hydrogel on addition of DOX (100 μM), OTC (100 μM) and TET (100 μM), respectively.

References

[1] Q. Cui, X. Wang, Y. Yang, S. Li, L. Li, S. Wang, *Chem. Mater.* **2016**, *28*, 4661−4669.

[2] S. Hussain, X. Chen, C. Wang, Y. Hao, X. Tian, Y. He, J. Li, M. Shahid, P. K. Iyer, R. Gao, *Anal. Chem.* **2022**, *94*, 10685–10694.

[3] X. Chen, S. Hussain, X. Chen, Y. Hao, P. Zhang, R. Gao, *Sens. Actuators B: Chem.* **2023**, *377*, 133081.

[4] A. H. Malik, S. Hussain, A. Kalita, P. K Iyer, *ACS Appl. Mater. Interfaces* **2015**, *7*, 26968−26976.